Optimum Design and 3D Finite Element Analysis of Non-slotted and Slotted Internal Rotor Type Axial Flux PM Disc Machines

M. Aydin**, Student Member, IEEE S. Huang*, T. A. Lipo**, Fellow, IEEE

* Department of Automation
Shanghai University
149 Yan-Chang Road
Shanghai, 200072, P.R.China

** Department of Electrical and Computer Engineering
University of Wisconsin-Madison
1415 Engineering Drive
Madison, WI 53706-1691, USA

Abstract: Axial flux internal rotor external stator surface mounted permanent magnet (AFIR) disc machines have simple structures, relatively high efficiencies and low cost. These machines can be used for the applications that require high power and torque density, high efficiency and low noise with the use of Neodymium Iron Boron magnets. In this paper, sizing equations of the AFIR machines are derived using generalized sizing equations. Optimum machine design is illustrated by choosing the diameter ratio and the airgap flux density. Using the optimum design data, field analysis of the slotless and slotted AFIR machines are investigated. Pulsating torque analyses are carried out using a 3D Finite Element Analysis (FEA) software. Minimization of cogging torque and ripple torque for both topologies is obtained using FEA utilizing the techniques such as modifying winding structure and skewing the rotor magnets. Finally the comparison of the two topologies in terms of torque quality is illustrated in the paper.

Keywords: Axial flux machine, PM machine, FEA, slotted and slotless machines, torque ripple, torque pulsations.

I. INTRODUCTION

AFIR type machines are slotless or slotted, toroidal-stator, external stator internal rotor, axial type permanent magnet brushless machines. They have experienced a growing interest recently for high performance drive applications [1-3] and can be designed for higher torque-to-weight ratio, higher efficiency and smooth torque.

Pulsating torque issues gain in importance for low noise and smooth torque applications for surface mounted PM disc machines. Pulsating torque comprises both cogging torque and ripple torque components. Cogging torque occurs from the variation of magnetic permeance of the stator teeth and the slots above the permanent magnets as the rotor rotates. The presence of cogging torque is a major concern in the design of permanent magnet machines since it adds unwanted harmonics to the pulsating torque. Ripple torque is mainly due to the fluctuations of the field distribution and the armature MMF which depends on the motor magnetic structure and the armature current waveform. Despite the fact that these torque components add unwanted harmonics to the pulsating torque, there exist certain techniques to minimize both cogging torque and ripple torque components of these disc type machines.

General sizing equations can be applied to AFIR topologies and optimum machine design with high power/torque density, high efficiency, low noise and smooth torque can be achieved [4-5]. In this paper, optimum design and field analysis of AFIR type machines, which have dual airgaps and stators, are investigated. First, structures of the non-slotted and slotted internal rotor type PM disc machines are reviewed. Second, the sizing analysis and optimum design of the topologies using generalized sizing equations [6-7] are introduced. Third, flux paths, flux densities on different portions of the machine and torque analysis including ripple and cogging torque components are analyzed using 3D Finite Element Analysis. Special attention is paid to torque ripple minimization using techniques such as using different winding structures and utilizing skewed rotor magnets. Finally, a comparison of the two structures and conclusions are presented.

II. AXIAL FLUX PM DISC MOTOR CONFIGURATIONS

The axial flux internal rotor external stator disc machine has a single rotor sandwiched between two stator discs. A typical axial flux slotless disc type PM motor (AFIR-NS) structure is shown in Figure 1.

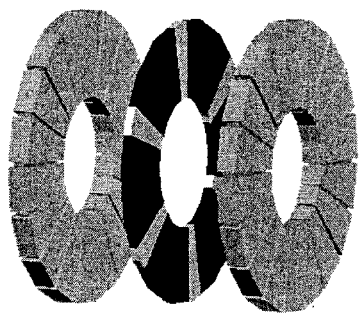

Fig. 1. Slotless internal rotor type axial flux machine structure

*Surong Huang was supported by Wisconsin Power Electronics Research Center and National Science Foundation of China (59877014).

The slotless AFIR machine has two stator discs and a single rotor disc. The stator of the machine is realized by slotless tape wound core with AC polyphase airgap windings that are back-to-back wrapped around the stator core. The rotor structure is formed by axially magnetized fan-shaped surface mounted Neodymium Iron Boron (NdFeB) permanent magnets and shaft. Detailed views of the stator and rotor structures of the AFIR-NS machine are given in Figure 2.

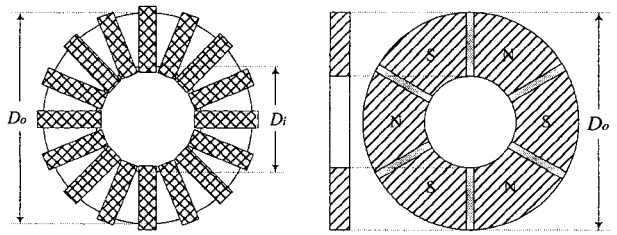

Fig. 2. Axial flux internal rotor type motor configuration a) slotless stator structure b) rotor structure

The portions between the windings are assumed to be filled with epoxy resin as in all non-slotted structures in order to increase the robustness of the structure and provide better conductor heat transfer. Moreover, the radial portions of the airgap windings are used for the torque production.

The slotted internal rotor type machine (AFIR-S) which is given in Figure 3 is realized by two slotted stators and a single PM rotor. The stator cores of the machine are formed by tape wound core with a lap and short-pitched polyphase AC winding located in punched stator slots. The winding pitch is designed to be 5/6 so that the airgap harmonics can be minimized. The rotor structure of the AFIR-S machine, which is the same as AFIR-NS machine rotor, is formed only by the axially magnetized NdFeB magnets where epoxy resin is used in between the magnets to form a solid rotor structure since there is no rotor disc to hold the magnets as in the disc type external rotor topologies.

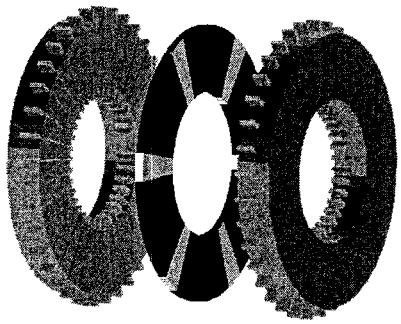

Fig. 3. Slotted internal rotor type disc machine model

The basic flux path of the two topologies is shown in Figure 4. As can be seen in the figure, the magnets with the polarity of N drive flux across the upper airgap into the upper stator core. The flux then travels circumferentially along the upper stator core, returns to the upper airgap, then enters the lower stator core through the S pole of the permanent magnets and closes its path. Flux directions of both slotless and slotted topologies at the average diameter in 2D are also shown in Figure 5a and 5b.

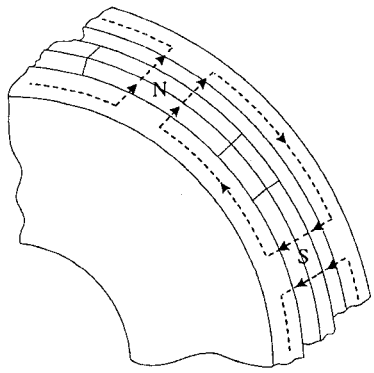

Fig. 4. 3D Flux paths of the AFIR topology

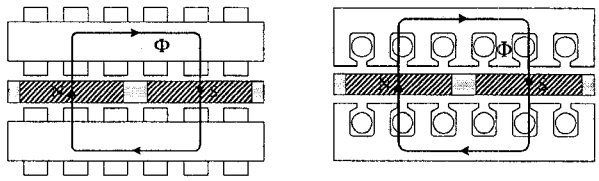

Fig. 5. One pole pair of the (a) non-slotted and (b) slotted AFIR type machines at the average diameter

III. DESIGN EQUATIONS OF THE AFIR TYPE MACHINES

An approach for a general purpose sizing equation has been developed in [4] and [5]. The sizing equation has the following form for axial flux machines (AFM):

$$P_R = \frac{1}{1+K_\phi}\,\frac{m}{m_1}\,\frac{\pi}{2}\,K_e K_i K_p K_L\,\eta B_g A\,\frac{f}{p}\,(1-\lambda^2)\frac{1+\lambda}{2}\,D_o^2 L_e \qquad (1)$$

where

P_R — rated output power of the machine,
$K_\phi = A_r/A_s$ — ratio of electrical loading on rotor and stator (without a rotor winding, $K_\phi = 0$),
m — number of machine phases,
m_1 — number of phases of each stator,
K_e — EMF factor
K_i — current waveform factor,
K_p — electrical power waveform factor,
η — machine efficiency,
B_g — air gap flux density,
A — total electrical loading,
f — converter frequency
p — machine pole pairs
L_e — effective stack length of the machine,
$\lambda = D_i/D_o$ — ratio of the diameter for the AFM.

D_o, D_g, D_i— machine diameters at outer surface, air-gap surface and inner surface,

$K_L=D_o/L_e$— aspect ratio coefficient for the AFM,

The outer surface diameter D_o From Eq. (1)

$$D_o=(2P_R/\frac{1}{1+K_\phi}\frac{m}{m_1}\frac{\pi}{2}K_e K_i K_p \eta B_g A \frac{f}{p}(1-\lambda^2)\frac{1+\lambda}{2})^{1/3} \quad (2)$$

The machine total outer diameter D_t for the AFIR type machines is given as

$$D_t = D_o + 2W_{cu} \quad (3)$$

where W_{cu} is the protrusion of the end winding from the iron stack in the radial direction and can be calculated as

$$W_{cu} = \begin{cases} \dfrac{D_i - \sqrt{(D_i^2 - A_s D_g)/K_{cu} J_s}}{2} & \text{for AFIR - NS} \\ \dfrac{(0.46 \sim 0.62) D_o}{p} & \text{for AFIR - S} \end{cases} \quad (4)$$

where K_{cu} is the slot fill factor of the stator winding and J_s is the current density of the stator winding.

The axial length of the machine L_e is

$$L_e=2L_s + L_r +2g \quad (5)$$

where L_s is axial length of the stator, L_r is axial length of the rotor and g is the air gap length. The axial length of a stator L_s is

$$L_s = \begin{cases} L_{cs} + 2W_{cu} & \text{for AFIR - NS} \\ L_{cs} + d_{ss} & \text{for AFIR - S} \end{cases} \quad (6)$$

where L_{cs} is the axial length of the stator core, and the depth of the stator slot for slotted machines d_{ss} is

$$d_{ss} = \frac{D_i - \sqrt{(D_i^2 - 2A_s D_g)/\alpha_s K_{cu} J_s}}{2} \quad (7)$$

where α_s is the ratio of stator teeth portion to the stator pole.

The axial length of the stator core L_{cs} can be written as

$$L_{cs} = \frac{B_g \alpha_p \pi D_o (1+\lambda)}{B_{cs} 8 p} \quad (8)$$

where B_{cs} is the flux density in the stator core and α_p is the ratio of average airgap flux density to peak airgap flux density.

Since there is no rotor core in internal rotor PM topologies, the axial length of rotor L_r is

$$L_r = L_{PM} \quad (9)$$

The PM length L_{PM} can be calculated as

$$L_{PM} = \begin{cases} \dfrac{2\mu_r B_g}{B_r - B_g K_f / K_d}(g + W_{cu}) & \text{for AFIR - NS} \\ \dfrac{2\mu_r B_g}{B_r - B_g K_f / K_d}(K_c\, g) & \text{for AFIR - S} \end{cases} \quad (10)$$

where μ_r is the recoil relative permeability of the magnet, B_r is the residual flux density of the PM material, K_d is the leakage flux factor, K_c is the Carter factor and K_f is the peak value corrected factor of air-gap flux density in radial direction of the disc motor.

IV. OPTIMIZATION OF THE AFIR TOPOLOGIES

In axial flux machines, the ratio, λ, and airgap flux density are the two important design parameters which have significant effect on the machine characteristics. Therefore, in order to optimize the machine performance, the ratio λ and the airgap flux density must be chosen carefully.

Figure 6 shows the power density variation as a function of airgap flux density and the ratio λ for the slotless AFIR machine.

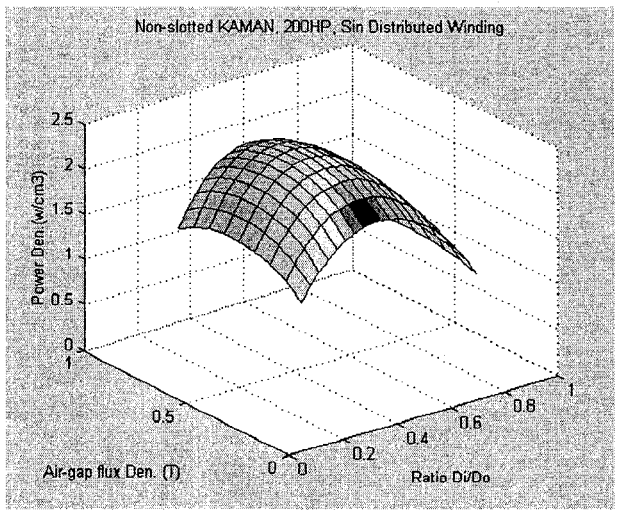

Fig. 6. Power density of AFIR-NS vs. air-gap flux density (B_g) vs. diameter ratio (λ)
P_R=200HP, n_s=1200rpm, p=3, A=600A/cm, J_s=6.6A/mm²

As can be seen from this plot, the maximum power density occurs at an airgap flux density of 0.58 T and the diameter ratio of λ=0.460. For that maximum power density point, the machine efficiency is 95.0%. The results are tabulated in Table 1.

Table 1. Optimization of the AFIR-NS machine for maximum power density point

Maximum power density (MPD)	P_{dmax}= 2.303 W/cm^3
Diameter ratio (λ) at MPD point	D_i/D_o=0.460
Airgap flux density at MPD point	B_g=0.58 T
Efficiency at MPD point	η = 95.0%

Optimization of the AFIR-NS machine can also be achieved for the maximum efficiency point. The maximum efficiency, which is 95.3%, occurs at a power density of 1.64 W/cm^3 and a ratio λ of 0.753. The efficiency of the machine does not change much as the diameter ratio changes (see Figure 8a).

Figure 7 shows power density plot as a function of airgap flux density and the ratio λ for the slotted AFIR machine.

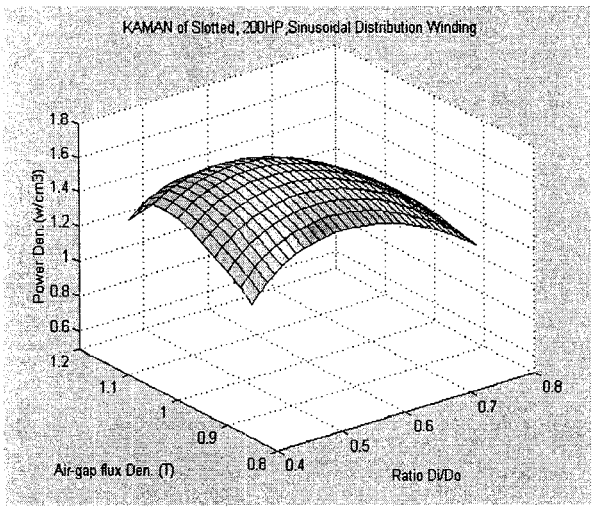

Fig. 7. Power density of AFIR-S vs. air-gap flux density (B_g) vs. diameter ratio (λ)
P_R=200HP, n_s=1200rpm, p=3, A=600A/cm, J_s=6.2A/mm^2

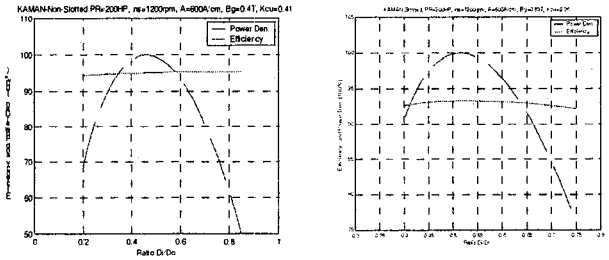

(a) (b)

Fig. 8. 2D view of the power density and efficiency plots for both (a) non-slotted and (b) slotted AFIR machines

From this plot, the maximum power density (or torque density), which is found as 1.777 W/cm^3, occurs at an airgap flux density of 0.99 T and the diameter ratio of λ=0.520. For that maximum point, motor efficiency is found to be 93.3%. Power density and efficiency plots in 2D view are also illustrated for both non-slotted and slotted internal rotor type axial flux PM machines in Figure 8.

V. 3D FIELD ANALYSIS AND FINITE ELEMENT CALCULATIONS

A. FEA of the Non-slotted AFIR Disc Machine

In order to analyze the magnetic circuit and torque pulsations, 3D Finite Element Analysis was used for both internal rotor type machines. The purpose of the FEA is to get the overall picture of the saturation levels in various parts of the machine, to compare the flux densities obtained from FEA and sizing analysis, and to investigate and minimize the cogging and ripple torque of both machines.

In non-slotted topology, the coils per pole per phase is chosen as 1 for each stator. In other words, there exist 18 back-to-back wrapped airgap windings around each stator. Sector shaped airgap windings are used in the model because of the fact that they provide better utilization of the stator core and help to reduce the torque ripple of the machine. Furthermore, skewed rotor magnets are used in the model. The pole arc ratio of the permanent magnets, α_i, was selected as 0.8. In other words, the ratio of the circumferential length of one PM to the circumferential length of one pole was 0.8. The machine parameters and important design dimensions used for the non-slotted machine model are shown in Table 2.

Table 2. Parameters and machine dimensions of non-slotted AFIR machine

Frequency (f)	60 Hz
Number of poles (p)	6 poles
Surface current density (A)	600 A/cm
Current density (J_s)	6.6 A/mm^2
Airgap length (g)	0.1 cm
Pole-arc-ratio (α_i)	0.8
Outer diameter (D_o)	78.69 cm
Inner diameter (D_i)	36.2 cm
Slot depth (d_{ss})	0 cm
Axial length of stator core (L_{cs})	3.41 cm
Axial length of rotor core (L_{cr})	0 cm
Magnet axial length (L_{pm})	2.12 cm

Figure 9 shows the airgap flux density of the machine for no load case. It can be seen from the plot that maximum airgap flux density is nearly 0.55T and the average airgap flux density is 0.42 T. It can also be noted from the airgap flux density plot that the flux density becomes greater at the edges of the magnets because of the fact that the leakage flux

between the magnets gains importance and causes high concentration of flux.

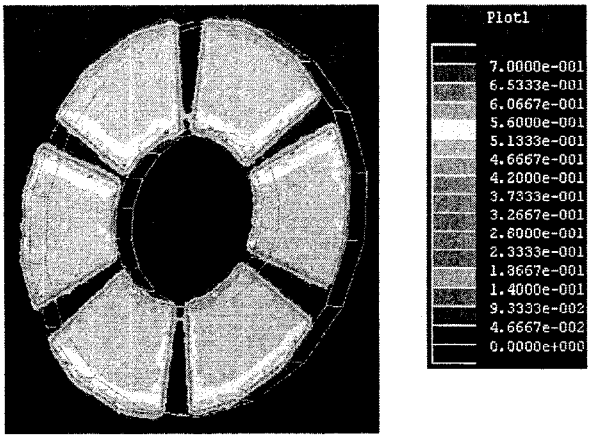

Fig. 9. Airgap flux density of the AFIR-NS machine at no load

The magnetization directions of the magnets were set in the 3D FEA program following the principle of the machine and is illustrated in Figure 10a. The flux directions in the airgap and stators of the machine for no load are also given in Figure 10b. The direction of the flux created by the magnets on the airgap and the direction of the flux traveling circumferentially along the stator cores can readily be noted from the figures.

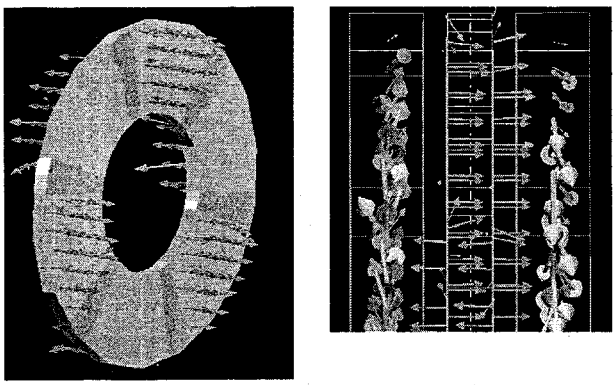

(a) (b)

Fig. 10. (a) Airgap flux density and (b) direction of the non-slotted AFIR machine at no load

A flux density comparison between the FEA results and sizing analysis results on various parts of the non-slotted disc machine at no load is tabulated in Table 3. The comparison table shows that the FEA results are consistent with the results obtained from the sizing analysis.

Table 3. Flux density comparison of non-slotted AFIR machine at no load

	Stator		Airgap	
	$B_{ts\text{-}max}$	$B_{cs\text{-}max}$	$B_{g\text{-}max}$	$B_{g\text{-}avg}$
FEA	0	1.75	0.55	0.42
Sizing A.	0	1.7	0.58	0.43

Figure 11 shows the airgap flux density over one pole using FEA. This curve shows that the flux density on the edges of the PM is about 15% higher than the flux density on the center of the PM because of the magnet leakage flux. Figure 12 illustrates how the airgap flux density of the non-slotted machine changes over one pole as the diameter varies from inner diameter D_i to outer diameter D_o.

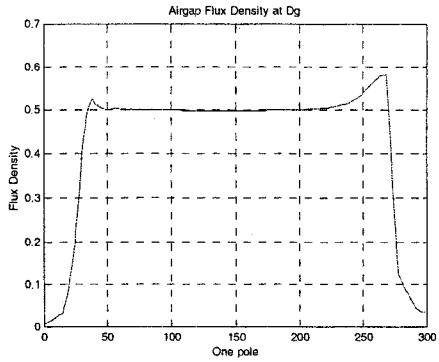

Fig. 11. No load airgap flux density of the axial flux internal rotor type non-slotted machine (at average diameter $D_g = (D_i + D_o)/2$)

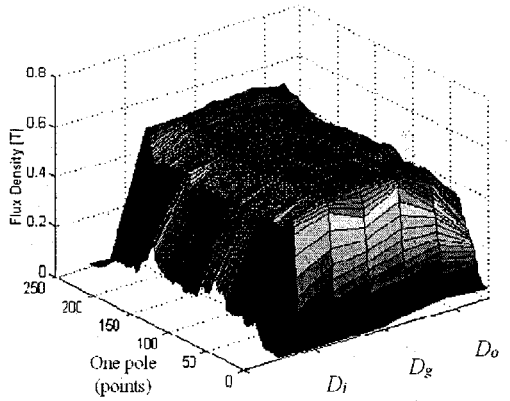

Fig. 12. No load airgap flux density of the axial flux internal rotor type non-slotted machine obtained from FEA (at D_i , D_g and D_o)

B. FEA of the Slotted AFIR Disc Machine

A FEA of the slotted axial flux internal rotor type PM machine was realized for both no load and rated load cases. The 5/6 short-pitched winding structure was used in the model for each stator. The slots per pole per phase is $q = 2$, which results in a 36 slot stator structure. The parameters and optimized machine dimensions used in the design which are calculated using sizing equations are shown in Table 4. Figure 13 shows the airgap flux density of the machine for the no load case. It can be seen from these plots that the maximum airgap flux density is roughly 1.0 T and the average airgap flux density was determined to be 0.75 T.

Table 4. Parameters and machine dimensions of slotted AFIR machine

Frequency (f)	60 Hz
Number of poles (p)	6 poles
Surface current density (A)	600 A/cm
Current density (J_s)	6.2 A/mm^2
Airgap length (g)	0.1 cm
Pole-arc-ratio (α_i)	0.8
Outer diameter (D_o)	53.09 cm
Inner diameter (D_i)	27.61 cm
Slot depth (d_{ss})	5.33 cm
Axial length of stator core (L_{cs})	5.12 cm
Axial length of rotor core (L_{cr})	0 cm
Magnet axial length (L_{pm})	1.90 cm

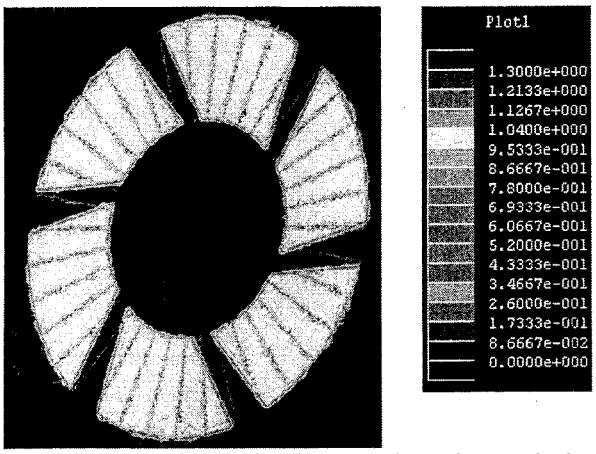

Fig. 13. Airgap flux density of the AFIR-S machine at no load

Using the principle of the internal rotor type axial flux PM machine, the magnetization directions of the magnets are set and the direction of the air gap flux density are illustrated in Figure 14 (a) while the flux directions in the stator of the machine at no load are shown in Figure 14 (b).

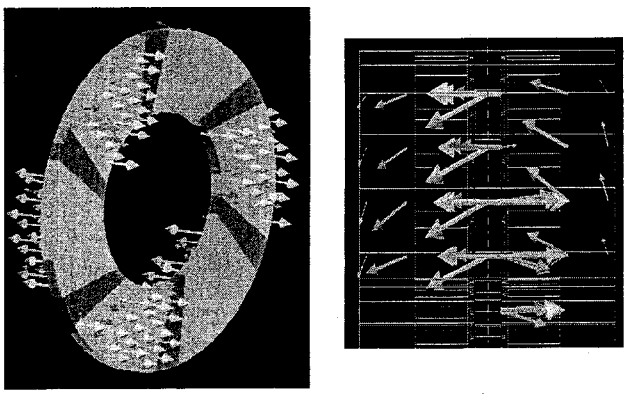

(a) (b)

Fig. 14. (a) Airgap flux density and (b) direction of the slotted AFIR machine at no load

A comparison of the flux densities between the FEA results and sizing analysis results for different parts of the machine at no load is tabulated in Table 5. From the no load flux density plots, it is seen that the results are again consistent with the results obtained from the sizing analysis. The maximum flux density values on the rotor and stator came out almost the same. Also, the maximum and average airgap flux densities obtained from the FEA and sizing analysis agree well.

Table 5. Flux density comparison of slotted AFIR machine at no load

	Stator		Airgap	
	$B_{ts\text{-}max}$	$B_{cs\text{-}max}$	$B_{g\text{-}max}$	$B_{g\text{-}avg}$
FEA	1.65	1.7	1.0	0.75
Sizing A.	1.8	1.7	0.99	0.74

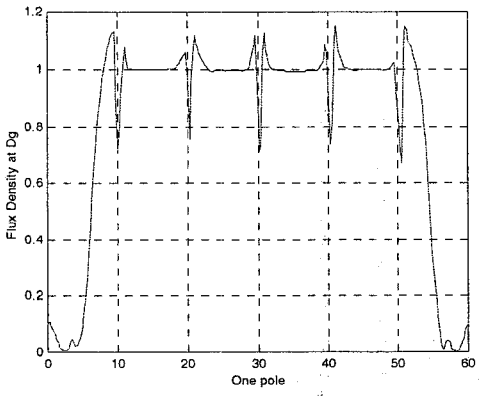

Fig. 15. Airgap flux density of the slotted machine obtained from FEA at average diameter D_g (With skewed PM case)

The airgap flux density at the average diameter (D_g) over one pole using FEA was obtained and is shown in Figure 15. This plot shows that there exist gaps in the airgap flux density right above the stator slots arising from the fact that there is a sudden change of the airgap permeance because of the slots. Figure 16 shows how the airgap flux density changes over one entire pole as the airgap diameter varies from inner (D_i) to outer (D_o). The flux density at the edges and in the middle portion of the PM as well as approximate slot openings can

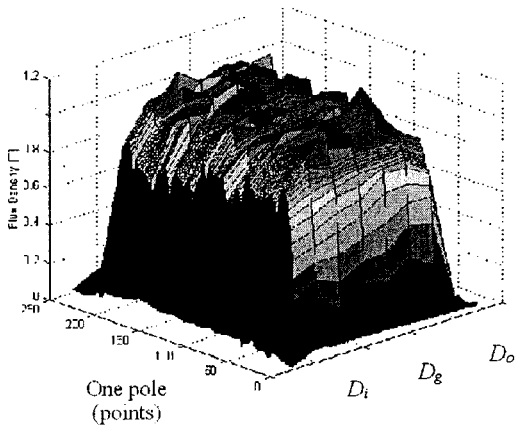

Fig. 16. 3D Airgap flux density for slotted AFIR machine obtained from FEA

clearly be seen from the 3D plot. Magnetic wedges could be used to help reduce the gaps, eliminate peaks and result in a smoother airgap flux density waveform but has not been incorporated into this analysis.

VI. TORQUE ANALYSIS USING FEA

In general, the total torque of a PM machine has three torque components: average torque, ripple torque and cogging torque. Since no slots exist in the non-slotted topology, the pulsating torque component of the machine is equal to the ripple torque component. However, in the slotted topology, pulsating torque comprises both cogging and ripple torque components.

A ripple torque analysis for the non-slotted internal rotor PM machine was accomplished for two different cases: a back-to-back (or gramme) type wrapped rectangular shaped winding with a non-skewed magnet case and a sector (or pie) shaped winding with a skewed magnet case. The main purpose of this analysis is to minimize the ripple torque of the machine using the techniques mentioned above. 3D Finite element calculations were completed in each case for different rotor positions over one pole to investigate the torque quality of the non-slotted machine. First, a torque ripple analysis was carried out for the back-to-back wrapped rectangular shaped winding. As can be seen from the total torque plot shown in Figure 17a, the torque ripple was found to be 0.105 pu. Second, the rectangular shaped windings were replaced with sector or pie shaped windings with skewed magnets and torque ripple analysis was repeated. The total torque of machine for pie shaped winding was plotted over one pole and is shown in Figure 17b. It can be seen that torque ripple was reduced to 0.055 pu. Thus, a torque ripple reduction from case 1 to case 2 was found to be 52%.

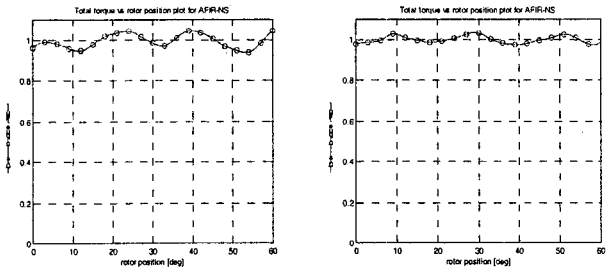

(a) (b)

Fig. 17. Total torque of the non-slotted internal rotor type machine (a) without and (b) with skewed rotor magnets

The cogging torque analysis of the slotted AFIR topology was carried out for two types of rotor structures: without and with skewed PM rotor. The resultant plots are given in Figures 18a and 18b. As can be seen from the cogging torque plots, the peak-to-peak cogging torque for the AFIR-S topology without skewing the magnets is 0.062pu. When the rotor magnets were skewed by 30 degrees, which is the optimum skew angle, the cogging became 0.013pu. Thus, skewing the PMs reduced the cogging torque of the slotted machine by 78.4%.

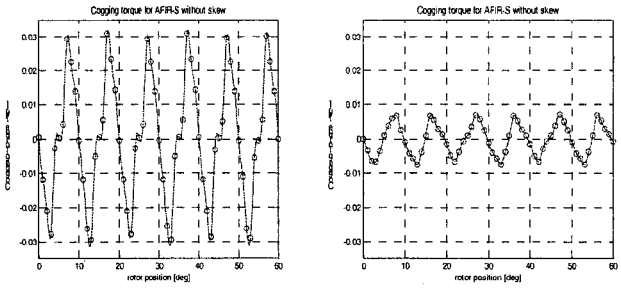

(a) (b)

Fig. 18. Cogging torque of the non-slotted internal rotor type machine (a) without and (b) with skewed rotor magnets

In order to obtain the total torque behavior of the slotted AFIR machine, 3D Finite Element calculations were performed for different rotor positions for non-skewed and skewed magnet cases. The pulsating torques of both types were plotted over one pole and are shown in Figure 19a and 19b. As can be seen from the plots, torque ripple has a peak-to-peak value of 0.383 pu for unskewed rotor case and 0.081 pu for skewed rotor case. This results in a ripple torque reduction of 78.7% by simply skewing the magnets.

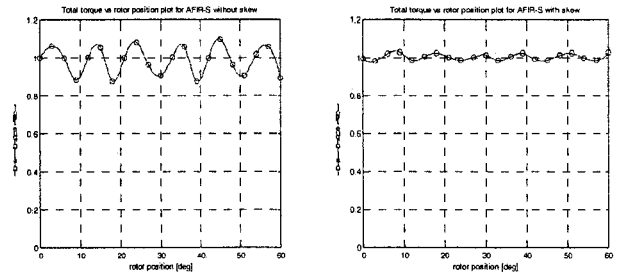

(a) (b)

Fig. 19. Total torque of the AFIR-S machine at rated load (a) without and (b) with skewed rotor magnets

VII. COMPARISON AND CONCLUSIONS

The focus of this paper has been to analyze the sizing of the axial flux internal rotor type PM topologies, to find the optimum machine design and to investigate the torque quality of both non-slotted and slotted AFIR type surface mounted PM machines. It was determined that in order to optimize the machine power density and efficiency, the ratio λ and the airgap flux density B_g must be chosen carefully. The magnet pole-arc ratio, the skew angle of the rotor magnets and winding distribution shape have to be chosen carefully to minimize the ripple torque as well.

3D FEA models have been developed to yield reasonable predictions of the torque quality and 3D field distribution of

both AFIR topologies. The machines were compared in terms of torque quality and the results were summarized in Table 6. First, cogging torque of the slotless AFIR type PM machine is not a concern due to the lack of stator slots. The peak-to-peak ripple torque of the machine was lessened to 5.5% by skewing the rotor magnets and using pie shaped stator windings. Second, the peak-to-peak cogging torque of the slotted machine was reduced from 6.2% to 1.3% of the rated torque. The cogging torque reduction by skewing the rotor magnets became 78.4%. Third, the peak-to-peak ripple torque of the slotted AFIR machine was reduced from 38.3% to 8.1% of the rated torque by simply skewing the rotor magnets resulting in 78.7% ripple torque reduction. Finally, the non-slotted AFIR topology has negligible cogging torque and lower ripple torque than its slotted counterpart.

Table 6. Ripple torque and cogging torque comparison for axial flux internal rotor type PM motor topologies

	Cogging Torque [pu]	Ripple Torque [pu]
AFIR-NS		
Rectangular	0	0.105
Pie shaped winding	0	0.055
AFIR-S		
Without skewed rotor	0.062	0.383
With skewed rotor	0.013	0.081

VIII. ACKNOWLEDGMENTS

The authors are grateful to the Office of Naval Research, the U.S. Army, for their financial support (Grant Number: N00014-98-1-0807).

IX. REFERENCES

[1] T. A. Lipo, S. Huang and M. Aydin, "Performance Assessment of Axial Flux Permanent Magnet Motors for Low Noise Applications", Final Report to Office of Naval Research, 2000, 450 pp.

[2] P. Mongeau "High Torque/High Power Density Permanent Magnet Motors", Proceedings of Naval Symposium on Electrical Machines, July 28-31, 1997, pp 9-16.

[3] S Huang, M. Aydin and T. A. Lipo, "A Direct to Electrical Machine Performance Evaluation: Part-2: Torque Quality Assessment", 2001 IEEE-IAS 36th Annual Meeting (pending).

[4] S. Huang, J. Luo, F. Leonardi, and T. A. Lipo, "A General Approach to Sizing and Power Density Equations for Comparison of Electrical Machines," IEEE Trans. on Industry Applications, IA-34, No.1, 1998, pp.92-97.

[5] S. Huang, J. Luo, F. Leonardi and T. A. Lipo, "A Comparison of Power Density for Axial Flux Machines Based on the General Purpose Sizing Equation", IEEE Trans. on Energy Conversion, Vol.14, No.2, June 1999, pp. 185-192.

[6] S Huang, M. Aydin and T. A. Lipo, "Comparison of (Non-slotted and Slotted) Surface Mounted PM Motors and Axial Flux Motors for Submarine Ship Drives", Third Naval Symposium on Electrical Machines, Dec. 2000.

[7] M. Aydin, S. Huang and T. A. Lipo, "Design and 3D Electromagnetic Field Analysis of Non-slotted and Slotted TORUS Type Axial Flux Surface Mounted Permanent Magnet Disc Machines," International Electrical Machines and Drives Conference, 2001, Boston (accepted for publication).

X. BIOGRAPHIES

Metin Aydin, a native of Turkey, received his B.S. degree in Electrical Engineering from Istanbul Technical University (ITU), Turkey, in 1993 and his M.S. degree in Electrical Engineering from the University of Wisconsin-Madison, WI, in 1997. He is presently a research assistant with WEMPEC (Wisconsin Electrical Machines and Power Electronics Consortium) and a Ph.D. student in Electrical Engineering at University of Wisconsin-Madison. His research interests include electrical machine design, control, electric drives, modeling and simulation. He is also a student member of IEEE and the vice president of the ITU Alumni Wisconsin Branch.

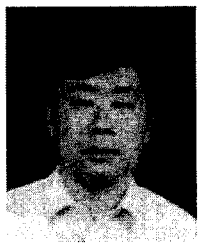

Surong Huang was born in Shanghai, China, in 1953. He graduated from Shanghai University of Technology, Shanghai, China, in 1977. In 1977, he joined the Shanghai University of Technology, Shanghai, China, as an Instructor Associate. He was promoted to Lecturer and Associate Professor at Shanghai University in 1987 and 1993, respectively. He was a Visiting Faculty Member in the Department of Electrical and Computer Engineering, University of Wisconsin- Madison in 1995-1996 and 1998-2000. He is engaged in research and development of new types of electrical machines and drive systems. His interests include design, control, and modeling of electrical machines and AC drives, vibration and noise analysis of electrical machines. He has published more than forty papers on these topics.

Thomas A. Lipo is (M'64-SM'71-F'87) is a native of Milwaukee, WI. From 1969 to 1979, he was an Electrical Engineer in the Power Electronics Laboratory, Corporate Research and Development, General Electric Company, Schenectady NY. He became a Professor of electrical engineering at Purdue University, West Lafayette, IN, in 1979 and, in 1981, he joined the University of Wisconsin, Madison, in the same capacity, where he is presently the W. W. Grainger Professor for power electronics and electrical machines.

Dr. Lipo has received the Outstanding Achievement Award from the IEEE Industry Applications Society, the William E. Newell Award of the IEEE Power Electronics Society, and the 1995 Nicola Tesla IEEE Field Award from the IEEE Power Engineering Society for his work. Over the past 35 years, he has served the IEEE in numerous capacities, including President of the IEEE Industry Applications Society.